# Technical note: Flow cytometry assays for the detection, counting and cell-sorting of polyphosphate-accumulating bacteria

Clémentin Bouquet[1], Hermine Billard[1,2], Cécile C. Bidaud[3], Jonathan Colombet[1,2], Young-Tae Chang[4], Karim Benzerara[3], Fériel Skouri-Panet[3], Elodie Duprat[3], Anne-Catherine Lehours[1]

[1]Université Clermont Auvergne, CNRS, LMGE, F-63000 Clermont-Ferrand, France
[2]UCA Partner, Cytometry, Sort and Transmission Electronic Microscopy (CYSTEM) platform, F-63000 Clermont-Ferrand, France
[3]Sorbonne Université, Muséum National d'Histoire Naturelle, UMR CNRS 7590 – Institut de Minéralogie, de Physique des Matériaux et de Cosmochimie (IMPMC), Paris, France
[4]Department of Chemistry, Pohang University of Science and Technology (POSTECH), Pohang 37673, Republic of Korea

Correspondence to: Anne-Catherine Lehours (a-catherine.lehours@uca.fr)

**Abstract.** In the context of the ecological sustainability of phosphorus (P), the emerging evidence of the ubiquitous presence of polyphosphate-accumulating bacteria (PAB) in natural environments invites efforts to reveal their unknown functions and roles in the biogeochemical cycle of P. This requires high-throughput methods to characterise PAB structure and dynamics in the environment. A promising strategy is to combine efficient staining of intracellular polyphosphate (polyP) granules in PAB and their subsequent detection by flow cytometry, enabling rapid data acquisition and multiparametric analysis. In this study, we provide a generic protocol for the detection, quantification, and cell sorting of PAB by flow cytometry using the dye 4'6-diamidino-2-phenylindole (DAPI). The assays were performed using *Tetrasphaera elongata,* which represent a large part of the microbial biomass in enhanced biological phosphate removal systems for wastewater treatment. We also included, as a negative control, a bacterial strain characterized by very low quantities of cellular polyP and carried out tests on water and lake sediment samples. We also show that the synthetic fluorochrome JC-D7, a new selective fluorescent dye used for the specific labeling of endogenous polyP in living cells, is promising for achieving these purposes, particularly in complex environmental samples.

## 1 Introduction

Since the 'green revolution' of the 1960s, the phosphorus (P) contained in geological deposits has been extracted in large quantities for the production of fertilisers, increasing the input of phosphorus to the biosphere fourfold compared with the pre-industrial era (Falkowski *et al.,* 2000). Over the same period, P storage in terrestrial and freshwater ecosystems increased dramatically (>75 %, Benett *et al.,* 2001). This excess P has led to a deterioration in ecosystem services, notably the formation of hundreds of coastal dead zones associated with eutrophication (Diaz and Rosenberg, 2008). Paradoxically, and by analogy with "peak oil", a "phosphorus peak" is predicted by 2035 (Cordell *et al.,* 2009; 2011). To ensure the ecological sustainability of P, holistic approaches that combine microbiology, ecology, and geochemistry are needed. In this vein, there is emerging evidence of the unexpected and ubiquitous presence of polyphosphate-accumulating bacteria (PAB) in natural environments such as rivers, lakes, and soils, inviting efforts to reveal their unknown functions and roles in the context of phosphorus availability and cycling (Rivas-Lamelo *et al.,* 2017; Akbari *et al.,* 2021; Bidaud *et al*., 2022).

40    Intracellular polyphosphates (polyP) are polymers containing from a few to hundreds orthophosphate residues linked together by phosphoanhydride bonds. Monovalent or divalent metal elements, such as $Mg^{2+}$, $K^+$, $Ca^{2+}$ and $Na^+$ can act as counterions in polyP polymers, forming complexes with the negatively charged phosphate residues (Akbari *et al.,* 2021). PolyP can account for up to 20 % of the dry weight of PAB as cells accumulate these polymers at cellular concentrations up to millimolar, for example, as an energy reserve to adapt and survive

45    environmental gradients or to scavenge nutrients (Martin *et al.,* 2014). PolyP accumulation in PAB can have an impact on P biogeochemistry, and PAB are expected to play critical roles as reservoirs or catalysts for P exchange between the geosphere and the biosphere (Diaz *et al*., 2008; Cosmidis *et al*., 2014); yet they are still missing from the global P cycle models. Unveiling the environmental significance of PAB and their effects on biogeochemical P cycle requires high-throughput methods to characterise their structure, dynamics, and function in complex and

50    heterogeneous environmental samples. To this end, a promising strategy is to combine the specific staining of intracellular polyP granules in PAB and their subsequent detection by flow cytometry (*e.g.*, Zilles *et al.*, 2002a; Günther *et al*., 2009; Terashima *et al.,* 2020).

Flow cytometry (FCM) is an essential tool in the field of environmental microbiology, enabling rapid data acquisition and multiparametric analyses. In combination with various dyes, FCM can be used to study

55    communities and analyse thousands of microbial cells per second. The ability of fluorescence-activated cell sorting (FACS) also makes FCM a powerful technique for identifying and isolating microbial cells with particular characteristics (Zilles *et al*., 2002a; Terashima *et al.,* 2020). Although FCM has already been applied to detect polyP fluorescence induced by different dyes (Zilles *et al*., 2002a; 2002b; Terashima *et al.,* 2020), there is still a lack of knowledge about optimal FCM parameters for the detection and counting of PAB from the environment.

60    In order to optimise detection and enumeration of PAB by FCM, we present here a detailed evaluation of a wide range of factors (storage conditions and staining specifications) likely to affect the quality of the fluorescent signal and therefore the efficiency of enumeration from DAPI staining of polyP. We also compare DAPI staining with that obtained with JC-D7, which is a benzimidazolinium dye. Although this novel polyP sensor has been shown to be suitable for staining polyP in living eukaryotic cells and tissues (Angelova *et al.,* 2014), it has not yet been

65    used to target PAB. The assays were performed using *Tetrasphaera elongata,* which represent a large part of the microbial biomass in enhanced biological phosphate removal systems for wastewater treatment. We also included, as a negative control, a bacterial strain characterised by very low quantities of cellular polyP and carried out tests on water and lake sediment samples. Our work provides a generic protocol for the detection, quantification, and cell sorting of PAB by FCM and highlights the JC-D7 dye as a promising fluorescent probe to achieve these

70    purposes, particularly in environmental samples.

## 2    Material and methods

### 2.1.   Strains and culture conditions

*Tetrasphaera elongata* Lp2 cells (DSM 14184) are gram-positive and are well known for accumulating large

75    amounts of intracellular polyP. Cells were grown in NM-1 medium (pH 7.1) containing (per litre): glucose (0.5 g); peptone (0.5 g); monosodium glutamate (0.5 g); yeast extract (0.5 g); $K_2HPO_4$ (0.44 g); $(NH_4)_2SO_4$ (0.1 g); $MgSO_4$, $7H_2O$ (0.1 g). A culture of a gram-negative strain named "RX" isolated at the Laboratoire Microorganismes: Génome et Environnement (LMGE), and identified as having a very small amount of

intracellular polyP, was used as negative control. RX cells were grown in PCA medium (pH 7) containing (per litre): tryptone (5.0 g); yeast extract (2.5 g) and glucose (1.0 g). Culture media were autoclaved (20 min, 121°C) and then filtered through Stericup® vacuum filtration systems with a porosity of 0.2 µm. Cultures (10 % vol/vol inoculum) were incubated at 28°C in Falcon® aerobic cell culture flasks with 0.2 µm hydrophobic membrane, in the dark, and shaken at 100 rpm. The kinetics of strain growth were monitored by measuring the optical density at 600 nm and subsequent analyses were performed during the exponential phase of growth.

**2.2. Environmental samples**

Sediment in the littoral zone of Lake Pavin (Auvergne, France) was sampled using a UWITEC (Mondsee, Austria) fitted with a polyvinyl chloride tube (1 m). The upper part (0-5 cm) of the sediment core was sampled using a sterile 50 mL pipette. To separate the microbial cells from the particles of sediment, 1 g of sediment was incubated for 30 min at 4 °C in 10 mL of sodium pyrophosphate buffer 0.01 M (pH 7.2) in a 15 mL Falcon® tube under agitation (280 rpm). The samples were placed for 1 min at 60 W in a sonication bath (Elmasonic S, Elma) and then centrifuged (2 min, 1500 g, 4 °C). The supernatant was collected and stored for 4 h at 4 °C until analysis. Water samples were collected in the water column of lake Pavin at 54 m depth with an 8-liter horizontal Van Dorn bottle.

**2.3. Properties of fluorescent dyes and preparation of staining solutions**

The 4'6-diamidino-2-phenylindole (DAPI), used at a final concentration of less than 1 µg.mL$^{-1}$ (Button and Robertson, 2001), is a fluorescent dye that strongly binds to DNA and the DAPI-DNA complex fluoresces blue, with a maximum emission at 460 nm, after excitation by an ultraviolet (UV, 350 nm) or violet laser (405 nm). DAPI also forms complexes with polyP when used at high concentrations (3-50 µg.ml$^{-1}$, Kulakova *et al.*, 2011). DAPI-polyP complexes emit yellow-green fluorescence (525–605 nm range; Allan and Miller, 1980) when excited by a violet laser. In the present study, a stock solution of DAPI (1 mg.mL$^{-1}$) was prepared according to the manufacturer's instructions (Thermo Fischer Scientific, Rockford, USA), aliquoted and stored at -20°C in the dark. The synthetic fluorochrome JC-D7 is identified as a polyP-specific marker (Angelova *et al.,* 2014). JC-D7 dye excited at 405 nm shows blue-green fluorescence emission between 480 and 510 nm. In this study, stock solutions (10 mM) of JC-D7 (Chemical Cellomics Laboratory, South Korea) were prepared in dimethyl sulfoxide (molecular biology grade DMSO, Merck, Darmstadt, Germany), aliquoted and stored at -20°C in the dark.

SYTO®62 fluorophore is a polymethine cyanine dye (cell permeable), that binds to nucleic acids. The DNA-SYTO®62 complex emits red fluorescence (676 nm) without spectral interaction with the polyP-DAPI or polyP-JC-D7 complexes, allowing the colocalization of DNA in PAB cells with polyP labelled with DAPI or JC-D7. In the present study, SYTO®62 stock solution (5 mM; Thermo Fischer Scientific, Rockford, USA) was stored at -20°C in the dark.

**2.4. Preparation of isotonic staining buffers**

The isotonic buffers used were as follows:

- Phosphate buffer saline (PBS; 1X; pH 7.2) containing per litre: NaCl (8 g); KCl (0.2 g); Na$_2$HPO$_4$ (1.44 g), KH$_2$PO$_4$ (0.24 g) and MilliQ® water qsp 1L.
- 4-(2-hydroxyethyl) -1-piperazine ethane sulfonic acid buffer (HEPES; 20mM, pH 7.4) containing per litre: 0.48 g of HEPES (Sigma Aldrich, CAS: 7365-45-9) and MilliQ® water qsp 1L.

- Tris hydrochloride and ethylenediaminetetraacetic acid buffer (Tris-EDTA; pH 7.4) containing 10 mM Tris-HCl solution and 1mM EDTA solution (Merck KGaA, Darmstadt, Germany).

- Citrate phosphate buffer (McIlvaine; pH 7.2) containing per litre: 869.5 mL of a 0.2 M $Na_2HPO_4$ solution; 115.5 mL of a 0.1 M citric acid solution and MilliQ® water qsp 1L.

120    Buffers were sterilized by filtration on 0.2 µM (Minisart® syringe filter, Sartorius).

### 2.5. Treatments tested to define the optimum conditions for polyP staining with DAPI

To establish the optimal conditions for intracellular polyP staining, *T. elongata* (TE) and RX cell culture samples were subjected to different treatments, including different DAPI concentrations (10 and 20 µg.mL$^{-1}$ final concentration) and incubation durations (30 and 60 min), types of staining buffer (PBS, HEPES, Tris-EDTA,

125    McIlvaine), percentages of fixative used (2 % and 4 % of formaldehyde Merck KGaA, Darmstad, Germany), storage temperatures (4°C, -20°C, -80°C) and time (1 h and 2, 7, 14 days), and detergent addition (0 and 0.3 % triton X100, Sigma CAS: 9002-93-1).

### 2.6. Flow cytometric (FCM) analysis of PAB after DAPI staining

The samples (final volume 200 µL) were analysed using a BD LSR Fortessa™ X-20™ flow cytometer (BD

130    BioSciences, San Jose, CA USA) in a three lasers configuration (405 nm, 50 mW; 488 nm, 60 mW; and 640 nm, 40 mW). Samples were diluted so that the event rate was less than 3,000 cell. s$^{-1}$. Fluorescence intensity, total cell number, forward scatter (FSC) and side scatter (SSC) were recorded. The fluorescence from DAPI-polyP (excitation at 405 nm) and SYTO®62-DNA (excitation at 640 nm) complexes was collected with 530/30 nm and 670/14nm bandpass filters, respectively. Data were acquired and analysed on logarithmic scales using

135    FACSDiva™ version 9.0 (BD Biosciences).

### 2.7. Fluorescence-activated cell sorting (FACS) enrichment of polyP-containing cell stained with DAPI

We analysed a water sample collected from 54 m depth in Lake Pavin and a culture sample of fresh mixture of *T. elongata* and RX (50/50 abundance). The samples were centrifuged (4000 g, 20 min, 4°C), resuspended in PBS solution, stained with DAPI (10 µg.mL$^{-1}$, 30 min in the dark) and SYTO®62 (1µM, 10 min) and immediately

140    processed. Analysis and cell sorting were performed with a BD FACSAria™ Fusion SORP cell sorter equipped with a 70 µm nozzle and a 1.5 neutral density filter (BD BioSciences, San Jose, CA USA) in a three lasers configuration (405 nm, 50 mW; 488 nm, 50 mW; and 640 nm, 100 mW). A forward scatter (FSC) threshold of 200 was used, and DNA was monitored using a 640 nm excitation laser and 670/30 nm emission filter. PolyP fluorescence was monitored using a 405 nm violet laser and a 525/50 nm emission filter. Cell sorting was

145    performed in purity mode and cells were sorted at a rate of approximately 1,500 cells. s$^{-1}$ into two fractions: polyP+ (high DAPI-polyP fluorescence) and polyP- (low or no DAPI-polyP fluorescence). Data were acquired and analysed on logarithmic scales using FACSDiva™ version 9.0 (BD Biosciences).

### 2.8. Observation by epifluorescence microscopy of intracellular polyP after labelling with DAPI

Samples were diluted with PBS (between $10^5$ and $10^6$ cells per sample), filtered through black polycarbonate

150    membranes (0.22 µm porosity, 25 mm diameter, GTBP, Millipore®) and stained for 30 min with DAPI (10 µg.mL$^{-1}$ final concentration). Filters were washed with 2 mL of PBS, incubated in the dark at 20 °C with DAPI (1 µg.

mL$^{-1}$, 10 min) or SYTO$^®$62 (1µM, 10 min) to visualise cellular DNA. After washing with 2 mL of PBS, the filters were dried and mounted with Immersol™ immersion oil (refractive index = 1.518, Zeiss). Cells were imaged using a Zeiss™ Axio Imager 2 microscope equipped with a FLUO COLIBRI 5 source with the following light-emitting
155   diodes: UV (385/30 nm), blue (469/38 nm), green (555/30 nm) and red (631/33 nm). The following bandpass filters were applied 450/50 nm, 525/50 nm and 690/50 nm for blue DAPI (DNA), green DAPI (polyP) and SYTO$^®$62, respectively. The diode intensity was adjusted as follows: DAPI blue 2%; DAPI green 100%; SYTO$^®$62 100%. PolyP and lipid inclusions are known to emit in the 450–650 nm range when excited at 360 nm, but lipid inclusions can be easily distinguished from polyP, as their fluorescence intensity is much lower and fades
160   rapidly within a few seconds (Terashima *et al.,* 2020). Therefore, all photographed images were exposed to excitation light for at least 1 min prior to imaging in order to detect consistent and long-lasting bright green-yellow fluorescence from the polyP. Three replicate counts were performed for each sample (between 200 and 1000 cells per sample). Images were acquired and processed on the Zen 3.3 blue edition.

### 2.9. Transmission electron microscopy coupled with energy dispersive x-ray (TEM-EDX) spectrometry

165   Samples were fixed with a 2% formaldehyde solution (final concentration) and collected on 400 mesh copper electron microscopy grids covered with a Formvar film (A03X, Pelanne Instruments, Toulouse, France) by centrifugation (18,000 g, 20 min, 14°C). After drying, the samples were observed and photographed using a JEOL JEM 2100-Plus transmission electron microscope (TEM), operating at 200 KV (JEOL Ltd, Tokyo, Japan), and equipped with a GATAN RIO 9M camera (Gatan Inc., Pleasanton, California, USA). Chemical elements were
170   analysed in the TEM (tilted to 20°) by energy dispersive X-ray (EDX) spectrometry using the X-Max 80 mm$^2$ Large Area SDD Silicon Drift Detector (Oxford Instruments, Abingdon-on-Thames, United Kingdom) equipped with the AZtec software (Oxford Instruments, Abingdon-on-Thames, UK), in point mode or map mode.

### 2.10. Comparison of polyP staining using DAPI or JC-D7 dyes

Samples were stained with JC-D7 for polyP detection (10 µg. mL$^{-1}$ final concentration, 30 min of incubation in
175   the dark, Angelova *et al.,* 2014) and with SYTO$^®$62 for DNA colocalization (1µM, 10 min, in the dark). The treatment used as a reference was polyP staining with DAPI (10 µg. mL$^{-1}$, 30 min in the dark). The FCM analysis was carried out as described in section 2.6 and the fluorescence of the JC-D7-polyP complexes (after excitation at 405 nm) was collected with a 530/30 nm bandpass filter (green fluorescence).

### 2.11. Controls and statistical analyses

180   For each experiment, unstained cells were used to establish FSC and SSC thresholds. Fluorescence thresholds for each dye (DAPI, JC-D7 and SYTO$^®$62) were achieved by independent staining. To avoid biases resulting from contamination or chemical interactions, we analysed each staining buffer alone, with each fluorochrome, or with a combination of dyes. Statistical analysis was performed using GraphPad Prism software, version 8.0.1 for Windows (GraphPad Software, La Jolla California, USA). The similarities between treatments were evaluated
185   using a one-way ANOVA, with Tukey's post-hoc test to make multiple comparisons between the groups or a t-test of Student for pairwise comparisons. The data were expressed as the mean ± standard error of the mean (mean ± SEM). A *p* value of less than 0.05 ($p < 0.05$) was considered as statistically significant.

## 3 Results

### 3.1. Microscopy observations of polyP granules and DAPI-polyP complexes

Transmission electron microscopy observations confirmed the presence of one or more intracellular electron-dense granules within the TE cells (Fig.1A). Although the distribution of carbon was relatively homogeneous within cells, energy dispersive x-ray (EDX) spectrometry revealed higher amounts of phosphorus and oxygen as well as the presence of monovalent ($Na^+$, $K^+$) and divalent cations ($Mg^{2+}$) in the granules (Fig. 1A, Fig. S1).

Observations by epifluorescence microscopy revealed highly refractive granules that emit fluorescence consistent with that expected for polyP after labelling with DAPI (Fig.1B and 1C). These observations confirm that the TE strain is a high accumulator of polyP (Fig. 1B), while the RX strain is a low accumulator (Fig.1C). The counting of DAPI-polyP complexes in epifluorescence microscopy will subsequently be used to validate the cytometric data.
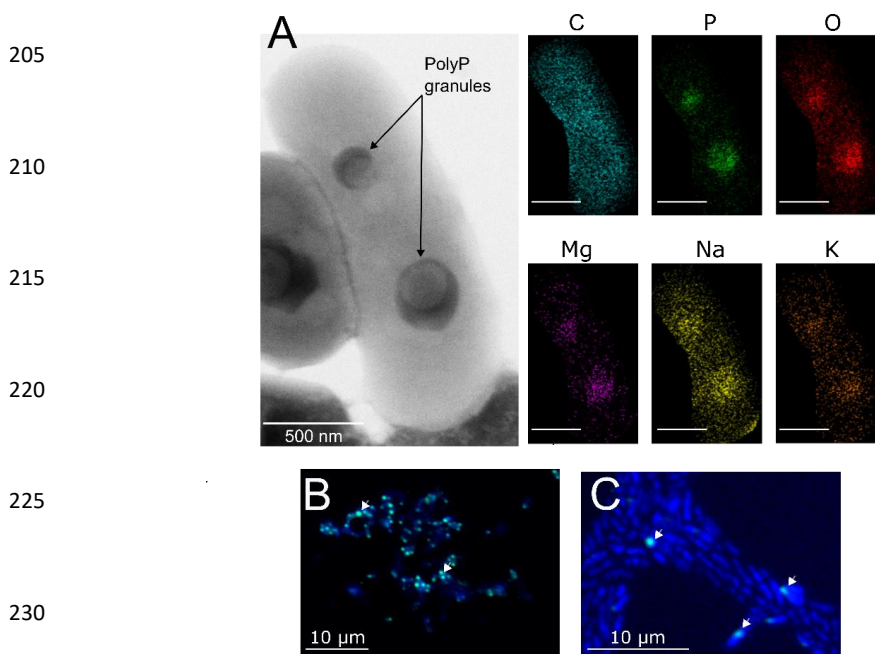
**Figure 1: Transmission electron microscopy coupled with energy dispersive x-ray spectrometry (TEM-EDX), and epifluorescence microscopy images of *T. elongata* and RX cells**.
(**A**) Representative image of two polyphosphate granules in a *Tetrasphaera elongata* Lp2 cell (DSM 14184) with EDX analysis indicating the chemical composition in and out of the granules. The elements shown are C for carbon (false blue colour), O for oxygen (false coloured in red), Na for sodium (red false colour), Mg for magnesium (false coloured in purple), P for phosphorus (green false colour), and K for potassium (false coloured in orange). Scale bars represent 500 nm (bottom left of photographs).
(**B**) and (**C**) DAPI-stained images by epifluorescence microscopy of *T. elongata* and RX cells, respectively. DNA and polyP emit a blue and a green-yellow fluorescence (examples are shown by white arrows), respectively.

245 **3.2. Isotonic buffer for labelling polyP with DAPI in flow cytometry (FCM)**

**3.2.1. Staining buffers versus population structure**

The effect of staining buffers on the TE and RX population structure was tested in the absence of labelling. The FSC and SSC parameters were analysed after 0, 10- and 20-min incubation in the following buffers: tris-EDTA, HEPES, PBS and McIlvaine. The Tris-EDTA buffer affected the structure of the RX population with the
250 differentiation of a subpopulation (P2) with incubation time (Fig. 2A), suggesting that tris-EDTA damaged the cellular integrity of RX cells. Therefore, Tris-EDTA buffer was excluded from further analyses.

**3.2.2. Staining buffers versus DAPI and SYTO®62 dyes**

The potential interference between dyes and isotonic buffers in the absence of cells was evaluated. No interference was observed between SYTO®62 and the HEPES, PBS, and McIlvaine buffers (data not shown). Negative controls
255 were also validated for DAPI in PBS and HEPES buffers (data not shown). However, artefact labelling was observed between DAPI and McIlvaine buffer, as evidenced by the detection of green fluorescent events in this cell-free buffer (Fig. 2B). The observed fluorescence was not related to microbial contamination, as demonstrated by the absence of events after labelling the McIlvaine buffer with SYTO®62 (data not shown). Therefore, the McIlvaine buffer was excluded from further analyses.
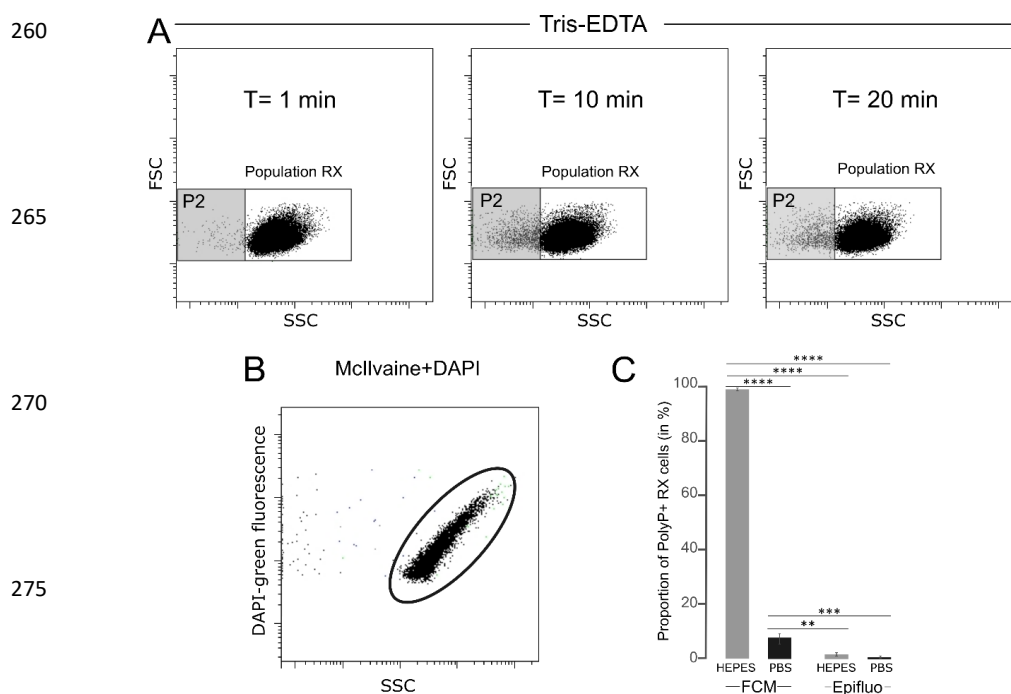
280 **Figure 2: Tests of different isotonic buffers for the labelling of polyP with DAPI in flow cytometry**
(**A**) Cytograms obtained after T=1 min, T=10 min and T=20 min incubation of unlabelled RX cells in Tris-EDTA buffer. (**B**) Cytogram obtained after DAPI labelling of McIlvaine buffer without cells revealing an artefact signal with green fluorescence. (**C**) Proportion of polyP+ cells counted by flow cytometry (FCM) or epifluorescence microscopy (Epifluo) after labelling RX cells with DAPI in HEPES or PBS buffer. Significance was determined using the Mann-Whitney test and one-way ANOVA
285 denoted as follows: $^{**}p < 0.001$, $^{***}p < 0.0005$, and $^{****}p < 0.0001$.
FSC: forward scatter, SSC: Side scatter

### 3.2.3. Staining buffers versus labelling performance

After labelling the TE cultures with DAPI (10 µg. mL⁻¹ for 30 min, Terashima *et al.,* 2020), the ratio of polyP+ cells (i.e. a strong green fluorescence signal) over the total cells of the TE strain was not significantly different regardless of the staining buffer (data not shown). However, the proportion of polyP+ cells detected in RX cultures using HEPES buffer (~99%) *vs* PBS (~1%) were very different (Fig. 2C). The control performed by epifluorescence microscopy after labelling the RX cells with DAPI, under the same conditions, showed that the correct ratio was that obtained in the PBS buffer (Fig. 2C). Consequently, the HEPES buffer was excluded from further analyses and PBS was used for the following FCM and FACS analyses.

### 3.3. Storage conditions and staining specifications

#### 3.3.1. Concentration and incubation time of DAPI

We tested two concentrations of DAPI (10 and 20 µg. mL⁻¹) and two incubation durations (30 min and 60 min). For TE and RX, the number of polyP+ cells detected was significantly higher for the 20 µg.mL⁻¹ DAPI / 60 min incubation treatment compared with the other three conditions (Fig.3A).

#### 3.3.2. Cell permeabilisation

To assess the degree of permeability on the efficiency of polyP labelling, RX and TE cells were pretreated with a synthetic detergent, triton X-100, or a fixative, formaldehyde. Cell incubation in 0.3 % triton X100 induced a cell loss of 43.5 ± 5.2 % and 62.7 ± 5.2 % for TE and RX, respectively, as revealed by the FSC and SSC cytometry data. After 1 h of incubation (T0), fixation with formaldehyde at a final concentration of 2 or 4% had an impact on the detection of polyP+ cells for the RX strain compared to unfixed culture (Fig. 3B). No significant differences in the number of polyP+ cells were observed for *T. elongata* fixed with 2 % and 4 % formaldehyde compared to unfixed cells (data not shown).
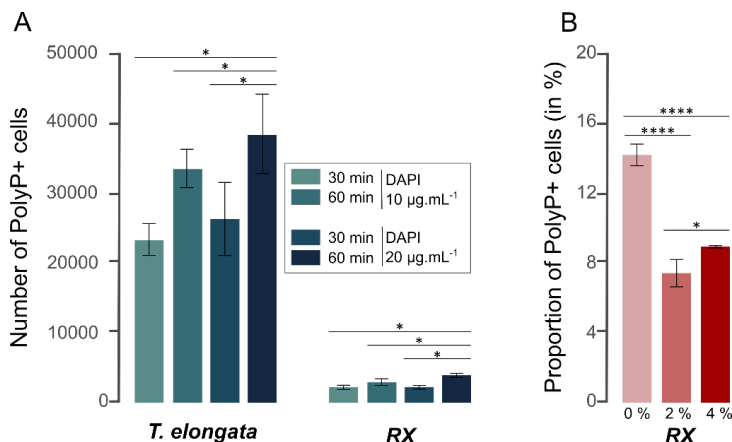
**Figure 3: DAPI-PolyP staining specifications and polyP+ cell preservation**
(**A**) Number of polyP+ cells detected by flow cytometry in *T. elongata* and RX cultures as a function of DAPI concentration (10 or 20 µg. mL⁻¹) and labelling time (30 or 60 min). (**B**) Proportion of polyP+ cells detected in the RX strain culture without addition of fixative (0%) and with 2% and 4% formaldehyde. Significance was determined using the Mann-Whitney test and one-way ANOVA denoted as follows: *$p < 0.05$, and ****$p < 0.0001$.

### 3.3.3. Cell preservation

PolyP preservation was assessed after formaldehyde fixation at different concentrations (2 or 4%), after different storage times (t = 2, 7 and 14 days) and at different storage temperatures (4 °C, -20 °C, -80 °C). Data were

330 expressed as the number of polyP+ cells detected compared to the number of polyP+ cells detected after 1 h of fixation (T0). No significant difference was observed for RX and TE strains, whatever the formaldehyde concentration, storage time or temperature (data not shown).

### 3.4. Validation of the DAPI-labelling protocol for polyP in TE and RX cell cultures

Fluorescence activated cell sorting (FACS) was performed on a mixture of TE and RX (50/50 relative abundance

335 (Fig. 4A). Prior to cell sorting, less than 40 % of cells were identified as polyP+ in the mixed TE+RX culture by FCM and epifluorescence (Fig. 4B). After cell sorting, $4.5.10^6$ and $4.3.10^6$ cells were collected in the polyP+ and polyP- fractions, respectively (Fig. 4C and 4D). A significant ($p<0.05$) enrichment in PAB was observed in the polyP + fraction, as shown by FCM and epifluorescence microscopy counts (Fig. 4E). By contrast, PAB represented less than 10 % in the polyP- fraction (Fig. 4F).

340
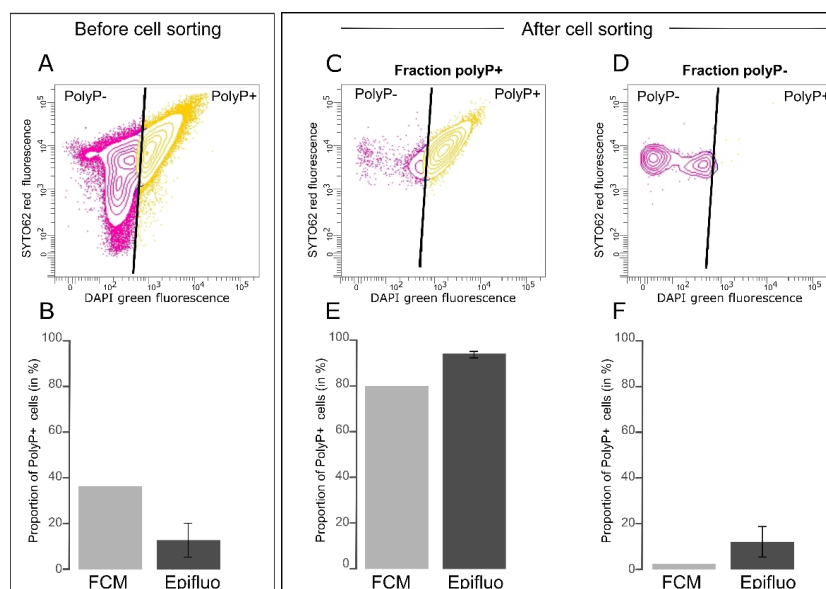
365 **Figure 4: PAB cell sorting from a mixed culture of *T. elongata* and RX**
(**A**) Cytogram showing the fluorescence of polyP-DAPI complexes (green fluorescence) and the fluorescence of DNA-SYTO62 complexes (red fluorescence) in the mixed culture of *T. elongata* and RX prior to cell sorting.
(**B**) Proportion of polyP+ cells in the mixed culture of *T. elongata* and RX, labelled with DAPI prior to cell sorting and counted by flow cytometry (FCM) and epifluorescence microscopy (Epifluo).
370 (**C**) and (**D**) Cytograms showing the fluorescence of polyP-DAPI complexes (green fluorescence) and the fluorescence of DNA-SYTO62 complexes (red fluorescence) in the (**C**) polyP+ and (**D**) polyP- fraction after cell sorting of the mixed culture of *T. elongata* and RX.
(**E**) and (**F**) Proportion of polyP+ cells in fractions (**C**) polyP+ and (**D**) polyP- after cell sorting of the mixed culture of *T. elongata* and RX and counted by flow cytometry (FCM) and epifluorescence microscopy (Epifluo).

375

### 3.5. Cell sorting and counting of PAB from environmental samples using DAPI

The protocol for labelling polyP with DAPI, validated on bacterial strains in this study, was applied to lake water
and sediment samples. After labelling DNA with SYTO®62 and polyP with DAPI, cells from a lake water sample
380 were sorted by flow cytometry and 7.9 x 10⁶ and 6.3 x 10⁶ cells were collected in the polyP+ and polyP- fractions,
respectively. Enrichment of targeted cells was observed in the polyP+ fraction, but this fraction contained only 52
± 1.8 % of PAB, as shown by control counts performed by epifluorescence microscopy (Fig. 5A). FCM analyses
of a sediment sample after double labelling SYTO®62-DNA and polyP-DAPI revealed an overestimation of the
proportion of PAB, since 75.8 ± 6.8% were counted by FCM, whereas only 12.3 ± 7% were counted by
385 epifluorescence microscopy (Fig. 5B).
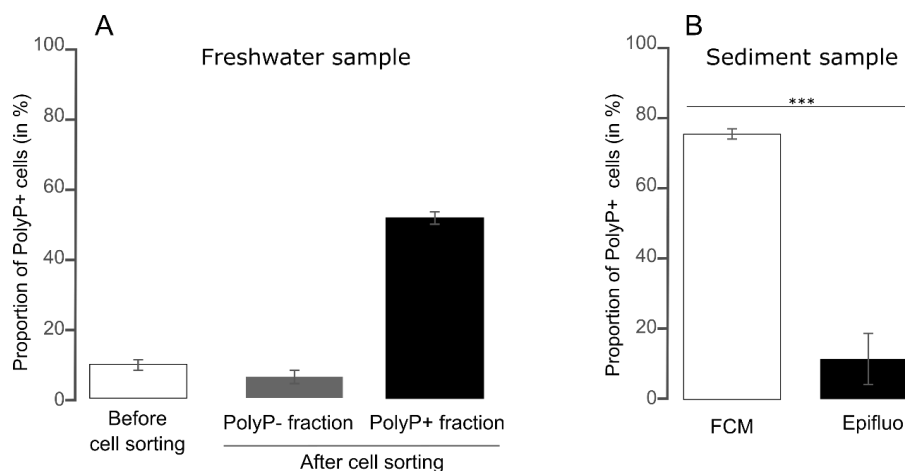
**Figure 5: PAB cell sorting and counting from freshwater samples**
**(A)** Proportion of polyP+ cells, after PAB labelling with DAPI and SYTO®62, in a water sample from Lake Pavin. Cells were
390 counted by epifluorescence microscopy in the sample before fluorescence activated cell sorting and, in the polyP, + and polyP-
fractions after cell sorting.
**(B)** Proportion of polyP+ cells in a sediment sample from Lake Pavin. Cell counts were carried out after PAB labelling with
DAPI and SYTO®62, using flow cytometry (FCM) and epifluorescence microscopy (Epifluo). Significance was determined
using the Student test and one-way ANOVA denoted as follows: ***$p < 0.001$.

395

### 3.6. Labelling of polyP with the fluorochrome JC-D7

Tests were performed with the JC-D7 dye for polyP labelling on TE and RX strains and on a lake sediment sample
under the experimental conditions as previously defined for eukaryotic cells (Angelova *et al.,* 2014). The green
fluorescence intensity of JC-D7 at 525 nm was found to be lower than that of DAPI for all samples analysed (data
400 not shown). The proportion of PAB identified after labelling with DAPI or JC-D7 was not significantly different
($p<0.05$) for TE and RX strains (Fig. 6). However, these two fluorochromes led to a different detection of polyP+
cells in the sediment sample by FCM (75.8 ± 6.8% and 5 ± 0.1% polyP+ cells for DAPI and JC-D7, respectively,
Fig. 6). Control counts by epifluorescence microscopy validated the proportions of polyP+ cells for the sediment
sample (12.3±7%), obtained by FCM after labelling with JC-D7 (Fig. 6).
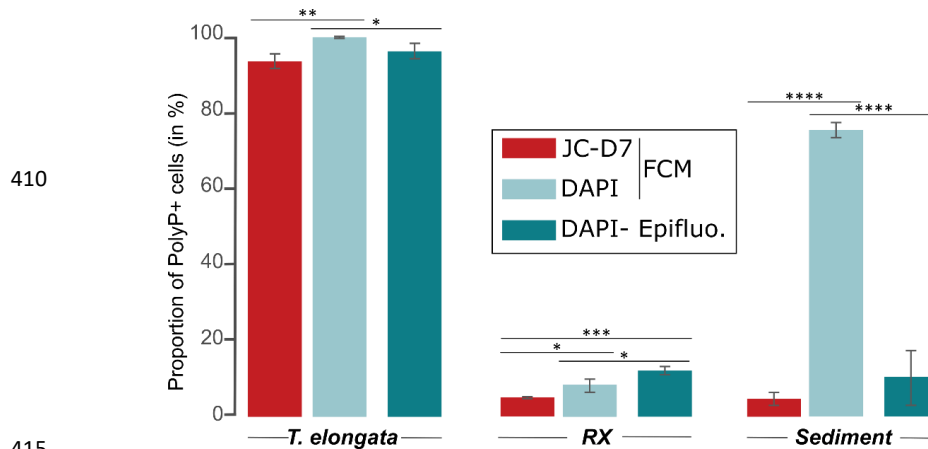
405

**Figure 6: Comparison of JC-D7 and DAPI labelling for PAB detection**
Proportion of polyP+ cells, after PAB labelling with DAPI and SYTO®62 or with JC-D7 and SYTO®62. Cells were counted by flow cytometry (FCM) or epifluorescence microscopy (Epifluo). Significance was determined using the Mann-Whitney test and one-way ANOVA denoted as follows: *$p < 0.05$, **$p < 0.001$, ***$p < 0.0005$, and ****$p < 0.0001$.

## 4 Discussion

Biogeochemical processes dependent on the accumulation of polyP in PAB have implications for the sustainable management of P resources. The present study established the basis of a robust protocol for the detection and enrichment of PAB by flow cytometry to eventually be able to acquire genomic and physiological data on new models of PAB and to characterise their distribution in natural environments at a high spatiotemporal resolution.

### 4.1. Optimisation of polyP labelling with DAPI

In the literature, the parameters for labelling polyP with DAPI were defined for use in epifluorescence microscopy (e.g. Mesquita *et al.,* 2013; Voronkov *et al*., 2019). Our data show that a specific adaptation of the labelling methods is necessary for the flow cytometry approach. For example, McIlvaine buffer, which has been identified to significantly enhance DAPI-polyP labelling in epifluorescence microscopy (Ray and Mukherjee, 2015), causes events with a size and structure that mimic nonviable cells. These artefact signals, linked to McIlvaine-DAPI interactions whose physicochemical origin is not identified, are revealed in this study, by flow cytometry. On the contrary, the intense fluorescence of DAPI-green during cell labelling performed in HEPES buffer suggests that the latter is an optimal solvent for the detection of polyP by flow cytometry. However, epifluorescence microscopy revealed an idiopathic and non-distinctive amplification of the DAPI staining of polyP+ and polyP- cells in this buffer. This study thus provides convincing evidence that the choice of buffer for labelling polyP with DAPI should be PBS, which is also a frequently used buffer for labelling DNA with this fluorochrome.

In addition, a protocol combining simplicity, practicality, and two essential conditions for high-throughput approaches and/or the analysis of a large number of samples, is proposed in this study for the detection of polyP by DAPI labelling. This protocol eliminates the need for laborious membrane permeabilisation steps, which did not amplify the expected signal in this study. On the contrary, significant losses were recorded in terms of the total

number of events and proportions of polyP+ cells with two compounds, a detergent (triton X100) and a fixative (formaldehyde), which have different modes of action but both permeabilize cell membranes. In order to reconcile

445 this methodological approach with the constraints of environmental studies, which often do not allow samples to be analysed immediately, the conservation of polyP was considered. The detection of bias-induced PAB immediately after formaldehyde fixation did not significantly increase after the samples were stored for 14 days at different temperatures (4°C, -20°C, -80°C). Consequently, we recommend storage, after fixation with 2% formaldehyde, at 4°C. This temperature avoids freeze-thaw cycles that could damage cells during repeated

450 analyses of the same sample. It is also compatible with transporting samples from the sampling site under *ad hoc* conditions.

In this study, we also applied the DNA-SYTO®62 and polyP-DAPI labelling simultaneously. This double labelling, which was not performed in previous studies (*e.g*., Günther *et al.* 2009; Terashima *et al.,* 2020), allows the separation of PAB from common contaminants such as organic matter aggregates. Furthermore, the choice of

455 SYTO®62 avoids interference with the metachromatic properties of DAPI by using a fluorochrome whose emission spectra are perfectly separable from the green and blue fluorescence of DAPI.

Controls were performed by epifluorescence microscopy, a standard method for quantifying and visualizing PAB (Serafim *et al*., 2002). We show that in the case of appropriate labelling (*e.g*., suitable staining buffer and dye), counts by epifluorescence microscopy and by FCM are of the same order of magnitude. The significant differences

460 sometimes observed may be due to the fact that FCM detects events that are difficult to distinguish with an epifluorescence microscope. To increase the precision of FCM measurements, it is necessary to carry out replicates in order to obtain average values that are not normally statistically different.

**4.2**. **JC-D7 fluorochrome specific to polyP as a prospective label for complex environmental samples**

465 Here the different conditions have been established to label polyP with DAPI, an inexpensive dye for which most epifluorescence microscopes and flow cytometers have combinations of excitation and emission filters compatible with the detection of its blue or green fluorescence (e.g. Tarayre *et al.,* 2016). The results we obtained in the mixture of TE+RX bacterial strains, using the FACS or FCM approach, demonstrated the efficacy of labelling polyP with DAPI in homogeneous matrices. Although the number of polyP+ cells detected using a high

470 concentration and incubation time of DAPI (20 µg.mL⁻¹, 60 min) is significantly higher (Fig. 3A), we recommend carrying out preliminary tests before increasing these parameters, as this may be due to the non-specific nature of DAPI staining. Indeed, the observations made by coupling polyP DAPI labelling with flow cytometry on the environmental samples highlighted that the lack of specificity of DAPI biased the FCM and FACS analyses. DAPI is a nonspecific polyP dye and, in addition to labelling DNA (blue fluorescence), it also interacts with lipids,

475 displaying metachromatic properties similar to those of polyP (Serafim *et al.,* 2002). Although the DAPI-lipid fluorescence is short-lived, with respect to the speed of flow cytometry analysis, it cannot be ignored.

The best option would therefore be to use markers specific to polyP, an approach that Gunther *et al.* (2002) have advocated. These authors proposed using the bright green fluorescence of the antibiotic tetracycline when it complexes divalent cations acting as a counthercharge in polyphosphate granules. Prior to the study presented here,

480 we had carried out assays by labelling cultured strains and/or environmental samples with tetracycline but had not obtained convincing results (data not shown).

Therefore, an exploratory analysis was performed to determine the potential of a heterocycle of the benzimidazole family for the detection of PAB in flow cytometry. The JC-D7 dye, identified as specific to polyP, has never been used to target PAB, but only for staining polyP in living eukaryotic cells and tissues. (Angelova *et al.,* 2014). The

485 data obtained in the present study show the specific nature of PAB labelling by this fluorochrome. Although its relevance to the study of polyp-hyperaccumulating prokaryotes needs to be confirmed by further studies, JC-D7 shows promise for greater reliability in detecting PAB in complex environmental samples.

**References**

490 Akbari A., Wang, Z., He, P., Wang, D., Lee, J., Han I. L., Li, G., and Gu, A. Z.: Unrevealed roles of polyphosphate-accumulating microorganisms. Microb. Biotechnol., 14, 82-87, doi: 10.1111/1751-7915.13730, 2021.

Allan, R. A., and Miller, J. J. : Influence of s-adenosylmethionine on DAPI-induced fluorescence of polyphosphate in the yeast vacuole. Can. J. Microbiol., 26, 912-920, doi.org/10.1139/m80-158, 1980.

Angelova, P.R., Agrawalla, B.K., Elustondo, P.A., Gordon, J., Shiba, T., Abramov, A.Y., Chang, Y.-T., and
495 Pavlov, E.V.: In situ investigation of mammalian inorganic polyphosphate localization using novel selective fluorescent probes JC-D7 and JC-D8. ACS Chem. Biol., 9, 2101–2110, doi.org/10.1021/cb5000696, 2014.

Aschar-Sobbi, R., Abramov, A. Y., Diao, C., Kargacin, M. E., Kargacin, G. J., French, R. J., and Pavlov, E.: High sensitivity, quantitative measurements of polyphosphate using a new DAPI-based approach. J. Fluoresc., 18, 859-866, doi: 10.1007/s10895-008-0315-4, 2008.

500 Bennett, E. M., Carpenter, S. R., and Caraco, N. F.: Human impact on erodable phosphorus and eutrophication: a global perspective: increasing accumulation of phosphorus in soil threatens rivers, lakes, and coastal oceans with eutrophication. BioScience, 51, 227–234, doi.org/10.1641/0006-3568(2001)051[0227:HIOEPA]2.0.CO;2, 2001.

Bidaud, C. C., Monteil, C. L., Menguy, N., Busigny, V., Jézéquel, D., Viollier, E., Travert, C., Skouri-Panet, F., Benzerara, K., Lefevre C. T., Duprat E.: Biogeochemical Niche of Magnetotactic Cocci Capable of Sequestering
505 Large Polyphosphate Inclusions in the Anoxic Layer of the Lake Pavin Water Column. Front Microbiol., 12, doi.org/10.3389/fmicb.2021.789134, 2022.

Button, D. K., and Robertson, B. R.: Determination of DNA content of aquatic bacteria by flow cytometry. Appl Environ Microbiol, 67,1636-45, doi: 10.1128/AEM.67.4.1636-1645.2001, 2001.

Cordell, D., Rosemarin, A., Schröder, J. J., and Smit, A. L.: Towards global phosphorus security: A systems
510 framework for phosphorus recovery and reuse options. Chemosphere, 84, 747-758, doi: 10.1016/j.chemosphere.2011.02.032, 2011.

Cordell, D., Drangert, J. -O., and White, S.: The story of phosphorus: Global food security and food for thought. Glob. Environ. Change, 19, 292–305, doi.org/10.1016/j.gloenvcha.2008.10.009, 2009.

Cosmidis, J., Benzerara, K., Morin, G., Busigny, V., Lebeau, O., Jézéquel, D., Noel, V., Dublet A. G., Othmane,
515 G.: Biomineralization of iron-phosphates in the water column of Lake Pavin (Massif Central, France), Geoch. Cosmoch. Acta, 126, 78-96. 10.1016/j.gca.2013.10.037, 2014.

Diaz, J., Ingall, E., Benitez-Nelson, C., Paterson, D., de Jonge, M. D., McNulty, I., and Brandes, J. A.: Marine polyphosphate: a key player in geologic phosphorus sequestration. Science, 320, 652-655, doi:10.1126/science.1151751, 2008.

520    Diaz, R. J., and Rosenberg, R.: Spreading dead zones and consequences for marine ecosystems. Science, 321, 926–929, doi :10.1126/science.1156401, 2008.

Falkowski, P., Scholes, R. J., Boyle, E., Canadell, J., Canfield, D., Elser, J., Gruber, N., Hibbard, K., Högberg, P., Linder, S., Mackenzie, T., Moore III, B., Rosenthal, Y., Seitzinger, S., Smetacek, V., and Steffen, W.: The global carbon cycle: a test of our knowledge of earth as a system. Science, 290, 291-296,
525    doi:10.1126/science.290.5490.291, 2000.

Günther, S., Trutnau, M., Kleinsteuber, S., Hause, G., Bley, T., Röske, I., Harms, H., Müller, S. Dynamics of polyphosphate-accumulating bacteria in wastewater treatment plant microbial communities detected via DAPI (4',6'-diamidino-2-phenylindole) and tetracycline labeling. Appl. Environ. Microbiol., 75, 2111-2121, doi:10.1128/AEM.01540-08, 2009.

530    Kulakova, A. N., Hobbs, D., Smithen, M., Pavlov, E., Gilbert, J. A., Quinn, J. P., and McGrath, J. W.: Direct quantification of inorganic polyphosphate in microbial cells using 4'-6-diamidino-2-phenylindole (DAPI). Environ. Sci. Technol. 45, 7799–7803, doi.org/10.1021/es201123r, 2011.

Martin, P., Dyhrman, S. T., Lomas, M. W., Poulton, N. J., and van Mooy, B. A. S.: Accumulation and enhanced cycling of polyphosphate by Sargasso Sea plankton in response to low phosphorus. PNAS 111, 8089– 8094, doi:
535    10.1073/pnas.1321719111, 2014.

Mesquita, D. P., Amaral, A. L., and Ferreira, E. C.: Activated sludge characterization through microscopy: A review on quantitative image analysis and chemometric techniques. Anal. Chim. Acta, 802, 14-28, doi.org/10.1016/j.aca.2013.09.016, 2013.

Mukherjee, C., and Ray, K.: An improved DAPI staining procedure for visualization of polyphosphate granules in
540    cyanobacterial and microalgal cells. Protocol Exchange. 10 (4075), doi:10.1038/protex.2015.066, 2015.

Rivas-Lamelo, S., Benzerara, K., Lefèvre, C. T., Monteil, C. L., Jézéquel, D., Menguy, N., Viollier, E., Guyot, F., Férard, C., Poinsot, M., Skouri-Panet, F., Trcera, N., Miot, J., and Duprat, E.: Magnetotactic bacteria as a new model for P sequestration in the ferruginous Lake Pavin. Geochem Perspect Lett, 5, 35-41, doi: 10.7185/geochemlet.1743, 2017.

545    Serafim, L. S., Lemos, P. C., Levantesi, C., Tandoi, V., Santos, H., and, Reis, M. A. M.: Methods for detection and visualization of intracellular polymers stored by polyphosphate-accumulating microorganisms, J. Microbiol. Methods 51, 1-18, doi.org/10.1016/S0167-7012(02)00056-8, 2002.

Tarayre, C., Nguyen, H. T., Brognaux, A., Delepierre, A., De Clercq, L., Charlier, R., Michels, E., Meers, E., and Delvigne, F. Characterization of phosphate accumulating organisms and techniques for polyphosphate detection:
550    a review. Sensors 16, 797, doi.org/10.3390/s16060797, 2016.

Terashima, M., Kamagata, Y., and Kato, S.: Rapid enrichment and isolation of polyphosphate accumulating organisms through 4'6-Diamidino-2-Phenylindole (DAPI) staining with fluorescence-activated cell sorting (FACS). Front. Microbiol. 11. doi.org/10.3389/fmicb.2020.00793, 2020.

555 Voronkov, A., and Sinetova, M. Polyphosphate accumulation dynamics in a population of *Synechocystis* sp. PCC 6803 cells under phosphate overplus. Protoplasma 256, 1153-1164, doi.org/10.1007/s00709-019-01374-2, 2019.

Zilles, J. L., Peccia, J., Kim, M. W., Hung, C. H., and Noguera, D. R. Involvement of Rhodocyclus-related organisms in phosphorus removal in full-scale wastewater treatment plants. Appl. Environ. Microbiol., 68, 2763-2769, doi: 10.1128/AEM.68.6.2763-2769.2002, 2002.

560 **Author contribution**

CB, HB, CCB, KB, F S-P, ED and ACL designed the work. CB, HB, Y-T C and ACL designed the experiments. ED was responsible for the research project (ANR Phostore). CB, HB, CCB, JC and ACL carried out the experiments. ACL and CB wrote the manuscript and all the authors revised it.

565 **Competing interest**

The authors declare that they have no conflict of interest

**Acknowledgments**

Clémentin Bouquet was supported by PhD fellowship from the French Ministry of Education and Research. Cécile Bidaud was supported by the Ecole Doctorale FIRE-Programme Bettencourt. The authors would also like to thank
570 Christopher Lefevre (BIAM, UMR 7265, CEA Cadarache) and Nicolas Menguy (IMPMC, UMR CNRS 7590, Sorbonne university). This work was supported by the Agence Nationale de la Recherche (PHOSTORE: ANR-19-CE01-0005). Young-Tae Tchang was supported by the National Research Foundation of Korea (NRF) grant funded by the Korea government (MSIT) (2023R1A2C300453411)

575 **Legends of figures**

**Figure 1: Transmission electron microscopy coupled with energy dispersive x-ray spectrometry (TEM-EDX), and epifluorescence microscopy images of *T. elongata* and RX cells**.

**(A)** Representative image of two polyphosphate granules in a *Tetrasphaera elongata* Lp2 cell (DSM 14184) with
580 EDX analyses indicating the chemical composition in and out of the granules. The elements shown are C for carbon (blue false colour), O for oxygen (false coloured in red), Na for sodium (red false colour), Mg for magnesium (false coloured in purple), P for phosphorus (green false colour), and K for potassium (false coloured in orange). Scale bars represent 500 nm (bottom left of photographs). **(B)** and **(C)** DAPI-stained images by epifluorescence microscopy of *T. elongata* and RX cells, respectively. DNA and polyP emit a blue and a green-
585 yellow fluorescence (examples are shown by white arrows), respectively.

**Figure 2: Tests of different isotonic buffers for the labelling of polyP with DAPI in flow cytometry**

**(A)** Cytograms obtained after T=1 min, T=10 min and T=20 min incubation of unlabelled RX cells in Tris-EDTA buffer. **(B)** Cytogram obtained after DAPI labelling of McIlvaine buffer without cells revealing an artefact signal with green fluorescence. **(C)** Proportion of polyP+ cells counted by flow cytometry (FCM) or epifluorescence microscopy (Epifluo) after labelling RX cells with DAPI in HEPES or PBS buffer.

FSC: forward scatter, SSC: Side scatter

**Figure 3: DAPI-PolyP staining specifications and polyP+ cell preservation**

**(A)** Number of polyP+ cells detected by flow cytometry in *T. elongata* and RX cultures as a function of DAPI concentration (10 or 20 µg.ml-1) and labelling time (30 or 60 min). **(B)** Proportion of polyP+ cells detected in the RX strain culture without addition of fixative (0%) and with 2% and 4% formaldehyde.

**Figure 4: PAB cell sorting from a mixed culture of *T. elongata* and RX**

**(A)** Cytogram showing the fluorescence of polyP-DAPI complexes (green fluorescence) and the fluorescence of DNA-SYTO®62 complexes (red fluorescence) in the mixed culture of *T. elongata* and RX prior to cell sorting.

**(B)** Proportion of polyP+ cells in the mixed culture of *T. elongata* and RX, labelled with DAPI prior to cell sorting and counted by flow cytometry (FCM) and epifluorescence microscopy (Epifluo).

**(C)** and **(D)** Cytograms showing the fluorescence of polyP-DAPI complexes (green fluorescence) and the fluorescence of DNA-SYTO®62 complexes (red fluorescence) in the **(C)** polyP+ and **(D)** polyP- fraction after cell sorting of the mixed culture of *T. elongata* and RX.

**(E)** and **(F)** Proportion of polyP+ cells in fractions **(C)** polyP+ and **(D)** polyP- after cell sorting of the mixed culture of *T. elongata* and RX and counted by flow cytometry (FCM) and epifluorescence microscopy (Epifluo).

**Figure 5: PAB cell sorting and counting from freshwater samples**

**(A)** Proportion of polyP+ cells, after PAB labelling with DAPI and SYTO®62, in a water sample from Lake Pavin. Cells were counted by epifluorescence microscopy in the sample before fluorescence activated cell sorting and, in the polyP+ and polyP- fractions after cell sorting.

**(B)** Proportion of polyP+ cells in a sediment sample from Lake Pavin. Cell counts were carried out after PAB labelling with DAPI and SYTO®62, using flow cytometry (FCM) and epifluorescence microscopy (Epifluo).

**Figure 6: Comparison of JC-D7 and DAPI labelling for PAB detection**

Proportion of polyP+ cells, after PAB labelling with DAPI and SYTO®62 or with JC-D7 and SYTO®62. Cells were counted by flow cytometry (FCM) or epifluorescence microscopy (Epifluo).